ELSEVIER

Journal of Alloys and Compounds 271–273 (1998) 123–127

Journal of ALLOYS AND COMPOUNDS

Determination of structural parameters of uranyl ions complexed with organic acids using EXAFS

M.A. Denecke[a,*], T. Reich[a], M. Bubner[a], S. Pompe[a], K.H. Heise[a], H. Nitsche[a], P.G. Allen[b], J.J. Bucher[b], N.M. Edelstein[b], D.K. Shuh[b]

[a] *Forschungszentrum Rossendorf e.V., Institute of Radiochemistry, P.O. Box 510119, D-01314 Dresden, Germany*

[b] *Lawrence Berkeley National Laboratory, Chemical Sciences Division, MS 70A-1150, Berkeley, Berkeley, CA 94720, USA*

Abstract

Two compounds of known crystal structure, sodium triacetatodioxouranium(VI), $Na[UO_2(CH_3COO)_3]$, and dibenzoatodioxouranium(VI), $UO_2[C_6H_5(COO)]_2$, were studied by uranium L_{III}-edge extended X-ray absorption fine structure, EXAFS, spectroscopy to differentiate between bidentate and monodentate coordination of carboxylate ions on the basis of the uranium–equatorial oxygen, O*eq*, bond lengths. Bidentate coordination can be verified by detecting carboxyl carbon atoms and the neighboring distal carbon atom of the organic rest. In contrast, EXAFS spectra for monodentate carboxylate complexes show no evidence of carbon atoms beyond the O*eq* coordination shell. The mode of coordination was determined by EXAFS analysis for solid uranyl complexes with humic, methoxybenzoic, and salicylic acids. A correlation between the U L_{III}-edge X-ray absorption near-edge structure, XANES, and the U–O*eq* bond distance according to the relationship $\Delta E \cdot R(\mathrm{O}eq)^2 = \mathrm{constant}$ was observed. For the samples studied, the constant was determined to be 197 ± 8 eV Å^2. © 1998 Elsevier Science S.A.

Keywords: Sodium triacetatodioxouranium(VI); Dibenzoatodioxouranium(VI); Extended X-ray absorption fine structure spectroscopy; Bidentate coordination; Monodentate coordination; Carboxylate ions

1. Introduction

We present results that show that the analysis of U L_{III}-edge extended X-ray absorption fine structure, EXAFS, data allows the differentiation of carboxylate ligands bound to uranium(VI) in a bidentate fashion from monodentate-coordinated carboxylate groups. Uranyl complexes with bidentate-coordinated carboxylate groups can be distinguished from their monodentate counterparts by their relatively long bond distances between uranium and equatorial oxygen atoms, O*eq* [1]. The near-collinear arrangement of the uranium, the carbonyl carbon atom, and the distal carbon, C*dis*, in the bidentate configuration leads to an enhancement of the EXAFS amplitude associated with C*dis* via multiple scattering, MS, effects. Therefore, detecting C*dis* atom(s) with EXAFS can substantiate the assignment of bidentate coordination [2]. In contrast, for monodentate-coordinated carboxylate groups it is often impossible to detect even the presence of carbonyl carbon atoms. Another linear grouping of atoms in uranyl complexes is found in the arrangement of the axial oxygen atoms, O*ax*, and uranium in the $[O{=}U{=}O]^{2+}$ unit itself. This leads to a MS peak in the Fourier transform, FT, of the EXAFS spectrum, appearing at twice the U–O*ax* bond length [3].

The EXAFS structural parameters for two uranyl carboxylates exhibiting either bidentate or monodentate coordination of the carboxylate ligands to uranium (see Fig. 1) were determined and compared to diffraction data: sodium triacetatodioxouranium(VI), $Na[UO_2(CH_3COO)_3]$ (**1**), [4] and dibenzoatodioxouranium(VI), $UO_2[C_6H_5(COO)]_2$ (**2**), [5]. EXAFS data from a uranyl humate (**3**) was then analyzed. Uranyl complexes with these organic macromolecules are of interest since humic acids, HAs, are prevalent in the environment and play a significant role in the migration/retardation of radionuclides in the geosphere [6]. In addition, spectra from two crystalline uranyl carboxylate compounds with yet unknown structure were analyzed: disalicylatodioxouranium(VI), $UO_2[C_6H_4(COO)(OH)]_2$ (**4**), and di-*o*-methoxybenzoatodioxouranium(VI), $UO_2[C_6H_4(COO)(OCH_3)]_2$ (**5**). The salicylato ligand was chosen because it contains both phenolic and carboxylate groups. These groups are pro-

---

[*] Corresponding author. Tel.: +49 351 2602012; fax: +49 351 2603553.

0925-8388/98/$19.00
PII: S0925-8388(98)00038-3

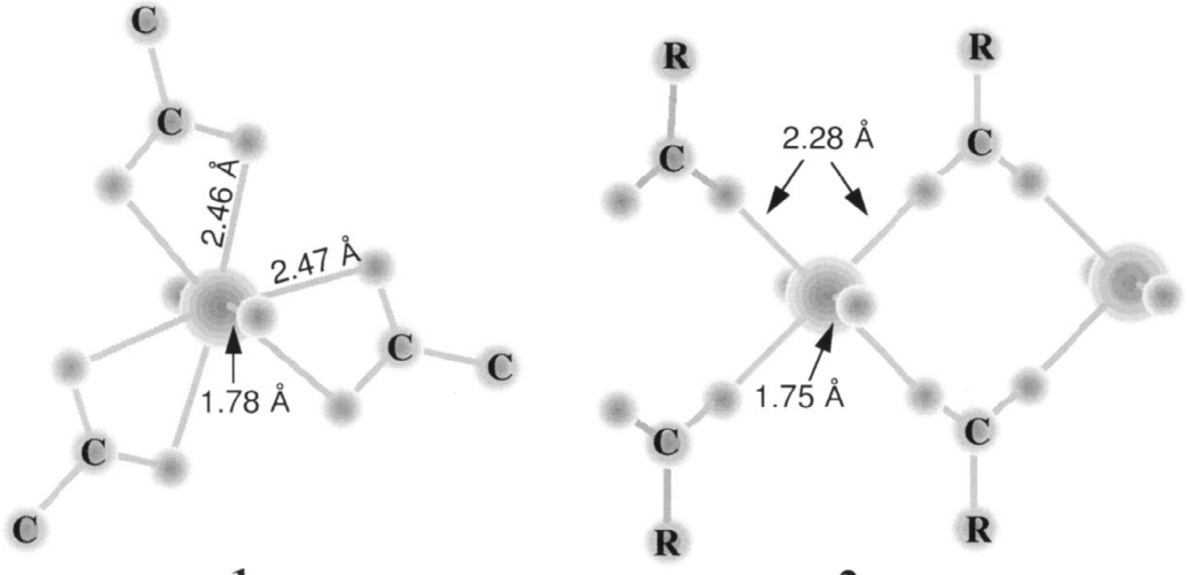

1 **2**

Fig. 1. Uranium (VI) coordination in sodium triacetatodioxouranium(VI), Na[UO$_2$(CH$_3$COO)$_3$] (**1**), and dibenzoatodioxouranium(VI), UO$_2$[C$_6$H$_5$(COO)]$_2$ (**2**). A neighboring uranyl unit in **2** is also shown to illustrate bridging of carboxylate ligands. Uranium, large spheres; C, carbon atoms; oxygen atoms, small spheres; R, benzene ring. Hydrogen atoms are omitted.

posed to be primarily responsible for the complexation of metal ions with HA [7]. The uranyl complex with the methoxy derivative was studied to ascertain any changes in the uranium coordination upon blocking the phenolic group.

2. Experimental

Sample **1** was prepared from diacetatodioxouranium(VI) dihydrate, UO$_2$(CH$_3$COO)$_2$×2H$_2$O (**6**), p.a. purchased from Merck, and sodium acetate according to Ref. [4]. The powder X-ray diffraction, XRD, diagram of the product agreed well with the theoretical diagram, with the exception of an unidentified peak at d=9.9 Å. *Anal*. Calc. (Exp.) %: C 15.3 (16.4), H 1.9 (1.8), Na 4.9 (6.8). The elemental analysis shows that the product contained nearly 0.5 mmol mg^{-1} of the sodium acetate reactant. Its presence, however, does not effect the EXAFS measurements. Sample **2** was prepared by reacting **6** with benzoic acid in a 1:2 stoichiometry. The acetic acid was distilled off from the reaction mixture, and the resulting product sintered at 130°C in a vacuum ampule in the presence of excess benzoic acid. Any non-reacted acid was removed via sublimation. The experimental XRD diagram was the same as the theoretical [5]. *Anal*. Calc. (Exp.) %: C 32.8 (32.8), H 2.0 (2.0). Sample **3** was prepared by reacting an aqueous suspension of solid natural HA from Fluka with uranyl nitrate solution as described in Ref. [8]. The loading of the humic acid proton exchange capacity, %PEC, with UO$_2^{2+}$ in **3** was determined to be 35% (assuming a charge neutralization reaction) using ICP-MS following digestion in HNO$_3$. Samples **4** and **5** were prepared by reacting UO$_2^{2+}$ with the corresponding acid, in a stoichiometric ratio of 1:2, in ethanol, at 60–65°C. *Anal*. Calc. (Exp.) %: (**4**) C 30.9 (30.6), H 1.9 (2.0); (**5**) C 33.5 (33.2), H 2.5 (2.6). Sample **4** was yellow-orange; all other samples (excluding sample **3**) were yellow.

Uranium L$_{\mathrm{III}}$-edge X-ray absorption transmission spectra of samples **1**, **2**, **4**, **5**, and **6** were measured at the Stanford Synchrotron Radiation Laboratory, SSRL (beamline 2.3) using a Si(220) double-crystal monochromator detuned ~50% of the maximum incident flux. The spectrum of sample **3** was recorded at the Hamburger Synchrotronstrahlungslabor, HASYLAB (beamline X1.1) using Si(311) crystals. The samples were dispersed in Teflon and pressed as 1.3-cm diameter pellets. Data reduction and analysis of averaged spectra from three scans for each sample were performed using the suite of programs EXAFSPAK [9] and standard techniques [10]. The energy axis of the spectra was calibrated against a reference spectrum, recorded simultaneously (a 0.2 M UO$_2$Cl$_2$ solution for HASYLAB spectra and either UO$_2$ or Y-foil for SSRL spectra). The ionization energy for the U L$_{\mathrm{III}}$-electron, E_0, was arbitrarily defined as 17185 eV for all averaged sample spectra.

Single scattering, SS, and MS amplitude and phase-shift functions were calculated with the theoretical EXAFS modeling code, FEFF7 [11], using a 21-atom cluster having the atomic positions from sample **6** [12]. The uranyl cation in this compound has both bidentate and monodentate carboxylate ligation, so that amplitude and

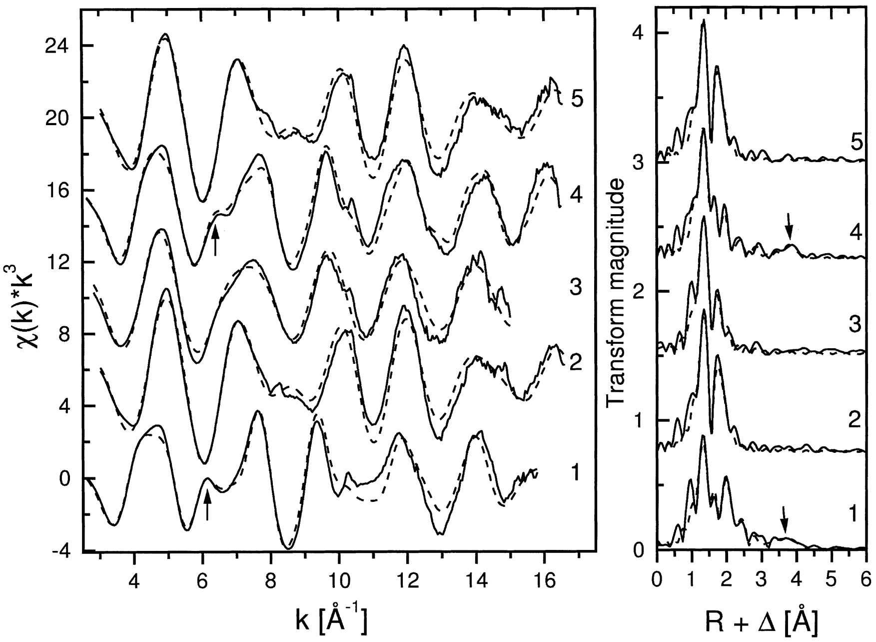

Fig. 2. Left: experimental k^3-weighted uranium L_{III}-edge EXAFS for samples **1**–**5** (———) and their corresponding fit as described in the text (- - -). Right: corresponding Fourier transforms (———) and their fit curves (- - -). Arrows mark features associated with bidentate-coordinated carboxylate ligands. For clarity, the spectra have been shifted along the *y*-axis.

phase-shift functions for oxygen and carbon atoms of both modes of coordination could be obtained in a single calculation.

3. Results and discussion:

The k^3-weighted U L_{III}-edge EXAFS oscillations, their corresponding Fourier transforms, FTs, and the theoretical fit curves for samples **1**–**5** are shown in Fig. 2. The EXAFS structural parameters are summarized in Table 1. To model the EXAFS for samples **2**, **3** and **5**, only the O*ax* and O*eq* shells and the uranyl MS path were needed. Samples **1** and **4** required inclusion of the carboxyl C and the C*dis* atoms in the fit. The C*dis* coordination shell was fit by a combination of the U–C*dis* SS path and both the three-legged (U→C→C*dis*→U) and four-legged (U→C→C*dis*→C→U) MS paths. Without these MS paths, the coordination number obtained for C*dis* was too large [2]. The fit of the C*dis* coordination shell in sample **1** was

Table 1
Bond distances, coordination numbers and Debye–Waller factors obtained from fits to the U L_{III}-edge EXAFS spectra of samples **1**–**5**

Sample	O*ax*		O*eq*			ΔE_0^a
	R (Å)	σ^2 (Å^2)	*N*	*R* (Å)	σ^2 (Å^2)	
1	1.78 [1.758]	0.002	5.2(4) [6]	2.48 [2.465]	0.006	−13.0
2	1.76 [1.749]	0.002	4.5(2) [4]	2.29 [2.281]	0.004	−8.5
3	1.78	0.002	5.3(5)	2.39	0.013	−8.0
4	1.77	0.001	5.6(6)	2.42	0.012	−10.5
5	1.77	0.002	4.4(2)	2.29	0.004	−8.5
	C			C*dis*		
	N	*R* (Å)	σ^2 (Å^2)	*N*	*R* (Å)	σ^2 (Å^2)
1	2.9(3) [3]	2.89 [2.853]	0.002	3(4) [3]	4.38 [4.349]	0.008
4	1.3(5)	2.86	0.003	1.4 [7]	4.29	0.002

Upper: parameters for axial and equatorial oxygen shells and ΔE_0 values for all samples. Lower: parameters for the carboxyl and distal carbon atoms of carboxylate groups in samples **1** and **4**. Uncertainties in the coordination numbers for the fit are given in parentheses. Values in brackets compare XRD results for **1** and **2** [4,5].

[a] ΔE_0 was held constant for all coordination shells at this value, obtained from fits to Fourier-filtered first two shell data.

[b] Three Na atoms were included in the fit yielding a distance of 4.0 Å with σ^2=0.03 Å^2.

somewhat complicated by the presence of three sodium atoms at a distance of 3.93 Å [4], which were included as an additional coordination shell with a constant coordination number of three. An alternative origin of the FT peak at 3.8 Å for sample **4** would be the presence of a strong backscatterer, i.e. uranium. However, carboxylate complexes with a U–U interaction around 4 Å show characteristic EXAFS features [13], which are lacking in the spectrum of sample **4**. Furthermore, the EXAFS of the Fourier-filtered peak at 3.8 Å could not be modeled by a U–U interaction. An illustration of the dissimilarity of amplitude and phases for the C*dis* MS paths and the U–U SS path is in Fig. 4 of Ref. [14].

In Table 1 the coordination numbers and bond distances of samples **1** and **2** are compared to XRD data. The coordination numbers and O*ax* and O*eq* bond distances obtained agree with the corresponding XRD values within 14% and 0.02 Å, respectively. The relatively long O*eq* bond lengths in samples **1** and **4** are indicative of bidentate carboxylate coordination. Three carbon atoms at distances of 2.89 and 4.38 Å are detected for sample **1**. These values are within 0.03–0.04 Å of XRD results. The large error of the C*dis* coordination number of sample **1** (see Table 1) is likely due to interference with the nearby sodium atoms (see above).

For sample **4**, the coordination numbers of the carboxyl carbon and C*dis* coordination shells are 1.4±0.7, indicating that only one to two bidentate coordinated carboxylate groups of the salicylate ligands are bound to uranium. The equatorial uranium shell of complex **4** consists of five to six O*eq* atoms. Sample **4** must contain linked UO_2^{2+} units in order to attain a 1:2 uranium to ligand coordination with five to six O*eq* atoms. Linking of UO_2^{2+} units via μ-oxo-bridges can be ruled out since no U–U interaction near 4 Å was detected. The presence of bridged UO_2^{2+} units, in addition to the one to two bidentate coordinated carboxylate groups, would presumably lead to a broad distribution of O*eq* bond lengths. This conclusion is supported by the large Debye–Waller factor, σ^2, of 0.012 for sample **4**. It should be noted that the U–C*dis* distance in sample **4** is 0.09 Å shorter than in sample **1**. This contraction is greater than expected from the shorter C–C bond distance in C_6H_5-COOH compared to CH_3-COOH.

The coordination of uranium in sample **5** must be the same as that in sample **2**. Both of these samples exhibit similar spectra, and the EXAFS analysis gave an identical U–O*eq* bond distance of 2.29 Å and identical coordination numbers. Blocking of the phenolic hydroxyl group of salicylic acid by a methyl group changes the mode of coordination of the carboxylic group from bidentate (sample **4**) to monodentate. In contrast to the bidentate complexes **1** and **4**, carboxyl carbon atoms in the monodentate complex **2** located at 3.46 Å [5] were not observed by EXAFS. The reason for this effect is discussed in Ref. [2].

The uranium atom in the uranyl humate **3** is surrounded by two O*ax* and approximately five O*eq* atoms at a distance of 1.78 and 2.39 Å, respectively. The U–O*eq* distance is in the range generally observed for monodentate-coordinated carboxylate groups [1]. Furthermore, no C*dis* atoms were observed for sample **3**. It can be concluded that the HA carboxylic groups responsible for the uranyl complexation act predominantly as monodentate, and not as bidentate, ligands when bound to the uranyl unit. This conclusion is supported by infra-red analysis of the carboxylate C–O stretches in samples **1**–**3**. The frequency difference between the asymmetric and symmetric carboxylate C–O stretches [$\nu_{as}(COO^-)-\nu_{sy}(COO^-)$] for the uranyl humate **3** is more than 140 cm^{-1} [8]. This value is comparable to that measured for the monodentate compound **2** (192 cm^{-1}), and much larger than that reported for the bidentate complex **1** (65 cm^{-1} [15]).

The U L_{III}-edge X-ray absorption near-edge structure, XANES, spectra of samples **1**–**6** are shown in Fig. 3. The position of the absorption maxima (white line, WL) has been aligned to compensate for the energy shift introduced by the different reference samples used. Two XANES features located approximately 10 and 35 eV above the WL are characteristic of all spectra. The nature of the first feature at 10 eV has been studied experimentally and theoretically and shown to originate from scattering off O*ax* atoms [3,16]. Since the U–O*ax* distance of all

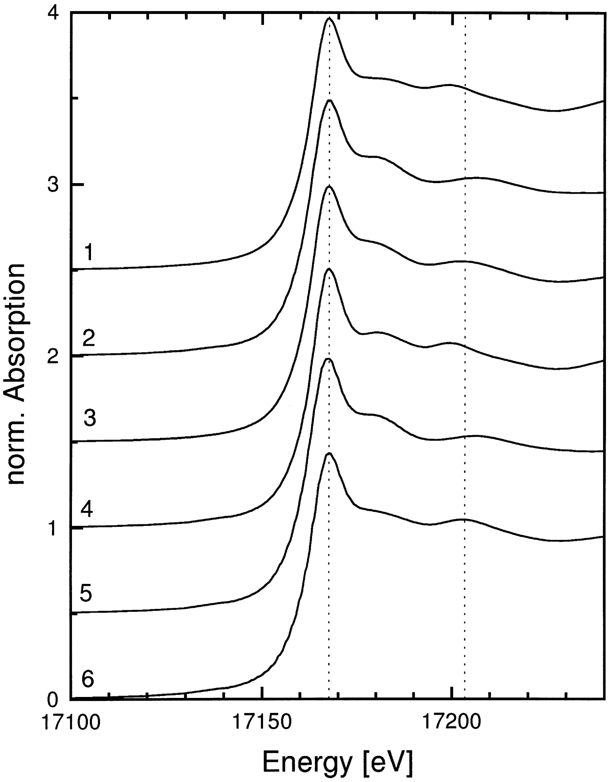

Fig. 3. Uranium L_{III}-edge XANES spectra for samples **1**–**6**. The dotted lines mark the white line, WL, maxima and the maximum of the feature about 35 eV above the WL for sample **6**. The spectra are shifted along the *y*-axis.

Table 2
The energy difference between the white line and the structure located near 17200 eV in the XANES spectra shown in Fig.3, ΔE, the U–O*eq* bond lengths, $R(\mathrm{O}eq)$, and the constant C, calculated as $\Delta E \cdot R(\mathrm{O}eq)^2 = C$: the mean value of C is 197 ± 8 eV Å^2

Sample	ΔE (eV)	$R(\mathrm{O}eq)^a$ (Å)	C (eV Å^2)
(**1**) $Na[UO_2(CH_3COO)_3]$	31.4	2.48	193
(**2**) $UO_2[C_6H_5(COO)]_2$	38.9	2.29	204
(**3**) Uranyl humate	34.4	2.39	196
(**4**) $UO_2[C_6H_4(COO)(OH)]_2$	31.4	2.42	184
(**5**) $UO_2[C_6H_4(COO)(OCH_3)]_2$	38.1	2.29	200
(**6**) $UO_2(CH_3COO)_2 \times 2H_2O$	35.7	2.39	204

[a] Values are from fits to EXAFS data, except for **6** where the value is from XRD results [12].

samples does not change significantly, the energy position of the resonance at 10 eV remains constant to within 0.7 eV.

A distinct correlation between the shape and energy position of the second XANES feature, located 35 eV above the WL, is observed. Measurement of polarized U L_{III}-edge XANES confirmed the assignment of this peak as originating from scattering of atoms in the equatorial plane [3]. The correlation between the energy position of this resonance and the U–O*eq* bond distance can be quantified using the well-known relation [17,18]: $\Delta E \cdot R^2 = C$, where ΔE is the energy separation between the maxima of the WL and the XANES feature, R is the bond length, and C is a constant. As can be seen from Table 2, the calculated C values for all samples are nearly identical. The average value for C of 197 ± 8 eV Å^2 can be used to estimate U–O*eq* bond lengths in uranyl carboxylates on the basis of measured ΔE values.

4. Conclusions

Uranium L_{III}-edge EXAFS analysis of several uranyl carboxylates showed that EXAFS is a valuable tool for differentiating between monodentate- and bidentate-coordinated carboxylate ligands. This method can be used to study the structure of uranyl complexes in solutions and amorphous solids, for example, environmentally relevant organic molecules such as humic acids.

The relation $\Delta E \cdot R(\mathrm{O}eq)^2 = 197 \pm 8$ eV Å^2 can be used to estimate U–O*eq* bond lengths, and thereby the mode of coordination, from XANES spectra. The change of the absorption coefficient in the XANES regime is much larger than in the EXAFS region. As a result, the XANES gives a stronger signal, so that structural information can be estimated for uranyl carboxylates species at concentrations so low that good-quality EXAFS spectra are unmeasurable.

References

[1] J. Leciejewicz, N.W. Alcock, T.J. Kemp, Structure Bonding 82 (1996) 44.
[2] M.A. Denecke, T. Reich, S. Pompe, M. Bubner, K.H. Heise, H. Nitsche, P.G. Allen, J.J. Bucher, N.M. Edelstein, D.K. Shuh, J. Physique IV 7 (1997) C2–637.
[3] E.A. Hudson, P.G. Allen, L.J. Terminello, M.A. Denecke, T. Reich, Phys. Rev. B54 (1996) 156.
[4] D.H. Templeton, A. Zalkin, H. Ruben, L.K. Templeton, Acta Crystallogr. C41 (1985) 1439.
[5] A. Cousson, J. Proust, M. Pages, F. Robert, E.N. Rizkalla, Acta Crystallogr. C46 (1990) 2316.
[6] R.J. Silva, H. Nitsche, Radiochim. Acta 70–71 (1995) 377.
[7] E. Tipping, M.A. Hurley, Geochim. Cosmochim. Acta 56 (1992) 3627.
[8] M.A. Denecke, S. Pompe, T. Reich, H. Moll, M. Bubner, K.H. Heise, R. Nicolai, H. Nitsche, Radiochim. Acta 79 (1997) 151.
[9] G.N. George, I.J. Pickering, EXAFSPAK: A suite of Computer Programs for Analysis of X-ray Absorption Spectra, Stanford Synchrotron Radiation Laboratory, Stanford, CA, USA, 1995.
[10] D.C. Koningsberger, R. Prins (Eds.), X-Ray Absorption: Principles, Applications, Techniques of EXAFS, SEXAFS and XANES, John Wiley & Sons, New York, 1988.
[11] S.I. Zabinsky, J.J. Rehr, A. Ankudinov, R.C. Albers, M.J. Eller, Phys. Rev. B52 (1995) 2995.
[12] J. Howatson, D.M. Grev, B. Morosin, J. Inorg. Nucl. Chem. 37 (1975) 1933.
[13] T. Reich, E.A. Hudson, M.A. Denecke, P.G. Allen, H. Nitsche, Poverkhnost 4-5 (1997) 149.
[14] P.G. Allen, D.K. Shuh, J.J. Bucher, N.M. Edelstein, T. Reich, M.A. Denecke, H. Nitsche, Inorg. Chem. 35 (1996) 784.
[15] N.W. Alcock, V.M. Tracy, T.C., Weddington, J. Chem. Soc. Dalton Trans. (1975) 2243.
[16] D.H. Templeton, L.K. Templeton, Acta Crystallogr. A38 (1982) 62.
[17] A. Bianconi, E. Fritsch, G. Calas, J. Petieau, Phys. Rev. B32 (1984) 4292.
[18] J. Petieau, G. Calas, D. Petitmaire, A. Bianconi, M. Benfatto, A. Marcelli, Phys. Rev. B34 (1986) 7350.